Extension of an automatic building extraction technique to airborne laser scanner data containing damaged buildings

Fayez Tarsha-Kurdi, M. Rehor, Tania Landes, Pierre Grussenmeyer, H.P Baehr

HAL Id: halshs-00264836
https://shs.hal.science/halshs-00264836

Submitted on 19 May 2008

EXTENSION OF AN AUTOMATIC BUILDING EXTRACTION TECHNIQUE TO AIRBORNE LASER SCANNER DATA CONTAINING DAMAGED BUILDINGS

F. Tarsha-Kurdi [a], M. Rehor [b], T. Landes [a], P. Grussenmeyer [a], H.-P. Bähr [b]

[a] Photogrammetry and Geomatics Group, MAP-PAGE UMR 694 – INSA de Strasbourg, 67000 Strasbourg, France - (fayez.tarshakurdi, tania.landes, pierre.grussenmeyer)@insa-strasbourg.fr
[b] Institute of Photogrammetry and Remote Sensing (IPF), Universität Karlsruhe (TH), Englerstr. 7, 76128 Karlsruhe, Germany – (miriam.rehor, hans-peter.baehr)@ipf.uni-karlsruhe.de

KEY WORDS: Laser scanning, LIDAR, Point Cloud, DSM, Segmentation, Extraction, Building, Disaster

ABSTRACT:

Airborne laser scanning systems generate 3-dimensional point clouds of high density and irregular spacing. These data consist of multiple returns coming from terrain, buildings, and vegetation. The major difficulty is the extraction of object categories, usually buildings. In the field of disaster management, the detection of building damages plays an important role. Therefore, the question arises, if damaged buildings can also be detected by a method developed for the automatic extraction of buildings. Another purpose of this study is to extend and test an automatic building detection method developed initially for first echo laser scanner data on data captured in first and last echo. In order to answer these two questions, two institutes share their data and knowledge: the *Institute of Photogrammetry and Remote Sensing* (IPF, Universität Karlsruhe (TH), Germany) and the *MAP-PAGE team* (INSA de Strasbourg, France). The used 3D LIDAR data was captured over an area containing undamaged and damaged buildings. The results achieved for every single processing step by applying the original and the extended algorithm to the data are presented, analysed and compared. It is pointed out which buildings can be extracted by which algorithm and why some buildings remain undetected.

1. INTRODUCTION

The airborne laser scanning technique represents a recent technology based on fast acquisition of dense 3D data and allowing the automation of data processing. Many applications have begun to find their way towards LIDAR data such as urban planning, GIS databases, mobile communication, and 3D city modelling or virtual reality. Among the LIDAR application domain, automatic building extraction and modelling have important positions. The former permits detecting building point clouds automatically from the total point cloud. During automatic building modelling, 3D building models which are composed of sets of intersected planes and edges are calculated. It has to be mentioned that a LIDAR system has the ability to capture many returns for every laser beam. For each of these returns the laser system generates one point cloud. So at the end of laser scanning many point clouds are provided whereas each one represents one return (Alharthy and Bethel, 2002). The most important of these point clouds are those belonging to the first and last returns. They are called first and last echo. Generally, the difference between first and last echo allows eliminating the vegetation from a digital surface model (DSM) during building extraction operations (Tarsha-Kurdi et al., 2006; Alharthy and Bethel, 2004; Tóvári and Vögtle, 2004). But in most cases, either last echo is less accurate than first echo (Hyyppä et al., 2005; Yu et al., 2005) or it is not separable from first echo (Pfeifer et al., 1999; Wotruba et al., 2005).

Nowadays, disaster management becomes more and more important. Due to the fast collection of height data, laser scanning is particularly suitable for the extensive coverage of information about the damage situation after disasters like earthquakes. As a consequence, damage analyses can be carried out rapidly after the occurrence of a disaster. This in turn can support rescue activities because the required resources depend among other things on the damage types appearing at the affected buildings (Schweier and Markus, 2004). Therefore, one project within the Collaborative Research Centre 461: "Strong Earthquakes: A Challenge for Geosciences and Civil Engineering" deals with the development of techniques for automatic determination of damage classes occurring at buildings in consequence of earthquakes (Rehor and Bähr, 2006). The project is sponsored by the *Deutsche Forschungsgemeinschaft* (German Research Foundation) and worked on by the *Institute of Photogrammetry and Remote Sensing* (IPF, Universität Karlsruhe (TH), Germany).

The classification of building damages will normally be based on the comparison of pre- and post-event building models. If no pre-event model is available, it might be helpful to know which buildings can be detected by a building extraction method based on laser scanning data. It is assumed that damaged buildings can only be recognised as buildings if their roof structure is preserved. So, if this presumption proves true, damage types like *outspread multi layer collapse* or any *heap of debris* type can be excluded for all buildings identified by the mentioned method. And although no statement can be made, if the buildings are damaged or not, it might be a useful hint for decision makers.

Due to these remarks, the *IPF* and the *MAP-PAGE team* (INSA de Strasbourg, France) are working together to answer the following two questions:

1. What are the benefits provided by the simultaneous use of first and last echo in an automatic building extraction operation?
2. Can damaged buildings be detected by a method developed for the automatic extraction of (undamaged) buildings?

2. RELATED WORK

Regarding automatic building extraction from LIDAR data, the proposed approaches can be divided into two families according to their processing manners. The first family presents approaches which are mainly based on images produced by interpolation and/or segmentation of the original point cloud. In this case, segmentation mostly means the generation of objects composed of similar pixels. The second family contains approaches trying to concentrate processing on point level. In this context, segmentation means the discrimination of several clusters in a point cloud. Another way to classify the automatic building extraction approaches can be achieved according to the used data: either they are using only first echo or first and last echo together.

This paper focuses on the latter classification, because its aim is to analyse if the consideration of two echoes is more appropriate than only one echo for the detection of damaged or undamaged buildings. In the approach family which uses first echo only, many methods are envisaged. The methods proposed by (Tarsha-Kurdi et al., 2006; Tarsha-Kurdi et al., 2007) suggest to superimpose the point cloud with the DSM and to analyse topological relationships between points located in the same cell for separating vegetation from buildings. (Whang and Tseng, 2004) propose the use of a segmentation based on an octree structure. Furthermore, the use of interpolation methods such as the linear prediction method (Kraus and Pfeifer, 1998; Rottensteiner and Briese, 2002) or the 3D surface detection (Lee and Schenk, 2002) can be cited.

In the second approach family which uses first and last echoes together, digital image processing techniques are employed, e.g. remote sensing classification methods (Tóvári and Vögtle, 2004; Lohmann and Jacobsen, 2004). In this category, two directions are followed: the first one considers the DSMs generated from first and last echo as two separate bands; the second one uses the first/last echo difference matrix as one single band. Another method developed by (Alharthy and Bethel, 2002) proposes the use of a gradient filter and the first/last echo difference matrix to eliminate vegetation.

Concerning the detection of damaged buildings after disasters, the use of laser scanning data is proposed in several publications, e. g. (Dash et al., 2004), (Vu et al., 2004a), (Vu et al., 2004b), (Murakami et al., 1999). But until now change detection methods based on LIDAR data have never been tested on data containing real damaged buildings.

3. DATA

The test site is a training field of the *Swiss Military Disaster Relief* located in the surroundings of Geneva (Figure 1). It is used for training search and rescue activities in case of catastrophic events and has a size of about 500 m × 800 m. It is situated in a valley and belongs to a hard-relief rural region. The particularity of the test area is that both undamaged and damaged buildings are located on it (Figure 1). Some characteristics of the buildings marked in Figure 1 are summarised in Table 2. The areas encircled in blue characterise damages like *outspread multi layer collapse* or different *heap of debris* types, whereas areas marked in red emphasise damage types like *pancake collapse* or *inclined planes*. As already mentioned in section 1, only the latter damage types are of interest since it is foreseeable that only such kinds of building

damages might be identified by an automatic building detection procedure.

In 2004 laser scanning data were acquired on the test site for the project within the Collaborative Research Centre 461 mentioned above. Table 1 contains some more information about the data.

For testing the developed algorithms, the first and last echo point clouds are considered. Furthermore, they enter into the processing chain in their original form (point cloud) as well as in their interpolated form (DSM).
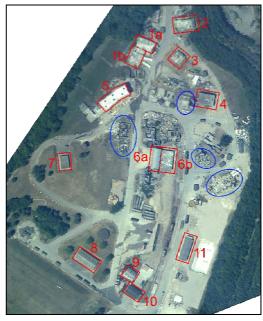

Figure 1: Aerial image of the test area (in red: undamaged buildings, pancake collapses, inclined planes; in blue: heaps of debris, outspread multi layer collapse)

Acqui-sition	Sensor	Flying height	Laser pulse rate	Scan width	Echo
June 2004	TopoSys Falcon II	900 m	83 kHz	14.3°	first and last

Table 1: Laser scanning data characteristics

4. THE ALGORITHMS

In automatic building extraction approaches, it is important to analyse the benefit provided by the simultaneous use of first and last echo in comparison with other methods using first echo only. In order to achieve this purpose, the method suggested by (Tarsha-Kurdi et al., 2006) which is based on first echo only has been tested by means of the available data. Moreover, this method has been extended to the use of both first and last echoes. Finally, a comparison of the results obtained by both methods is carried out.

4.1 Building detection using first echo only

As aforementioned, the method developed by (Tarsha-Kurdi et al., 2006) is initially based on the first echo point cloud and the DSM derived from it by nearest neighbour interpolation. The

last echo point cloud is not included in the workflow because it is not always available with a sufficient reliability. The approach consists of two steps: the segmentation of the point cloud into terrain and off-terrain points, and then the extraction of a building subclass from the off-terrain class.

The first step uses only the DSM as input data. Furthermore two thresholds Δh and S are introduced, where Δh represents the minimum height difference between terrain and off-terrain and S typifies the minimal acceptable building surface. In order to carry out this processing step, successive procedures are achieved. Firstly, the borders of the off-terrain class are detected using gradient filters and the threshold Δh. Secondly, the bodies of the segment borders created previously are filled by means of an algorithm which uses a 3×3 moving window passing over the binary matrix containing the off-terrain borders.

The second stage consists in the discrimination of the off-terrain into vegetation and buildings. The input data of this step are the calculated off-terrain mask containing all off-terrain objects, the DSM and the original point cloud. This operation starts with the detection of the building kernels by studying the spatial topological relationships between points included in the same cell of the DSM. Afterwards a region growing algorithm is carried out starting from these extracted kernels to identify the remaining building points. During this operation based on the DSM only, two thresholds S and Δh_{roof} are adopted. The first one (S) represents again the minimal acceptable building surface and the other one (Δh_{roof}) typifies the maximum allowed roof slope converted into a height difference by means of the DSM sampling value p (p=1 m) (Tarsha-Kurdi et al., 2007).

4.2 Building detection using first and last echo

In this section, the algorithm described previously is extended to the use of first and last echo. Before presenting the main elements of the extended approach, it is necessary to define the DIF matrix.

4.2.1 Calculation and analysis of the DIF matrix: The DIF matrix expresses the difference between first and last echo and is calculated by the subtraction of the two DSMs (eq. 1).

$$DIF = DSM_{FE} - DSM_{LE} \qquad (1)$$

where DSM_{FE} = DSM generated from first echo
         DSM_{LE} = DSM generated from last echo

Figure 2 shows the DIF matrix and emphasizes that the values of the pixels are located between –20 m and +20 m. The majority of the non-null pixels have positive values. This confirms the fact that the first echo captures points located on a higher altitude than the last echo.

By analysing the DIF matrix values in more detail three main intervals can be extracted:

1. Pixels with positive values (10.7 % of the total number). They represent vegetation and building borders. Sometimes they represent noise.
2. Pixels with values equal zero (86.0 %). They represent terrain and building bodies. Only a few points are located in vegetated areas.
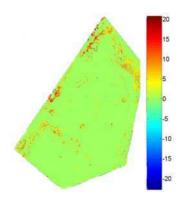3. Pixels with negative values (3.3 %).

Figure 2: Visualisation of the DIF matrix

The presence of the last kind of pixels can be explained easily. A pixel of negative value does not result from the same laser beam in first and last echo. For example, Figure 3 presents three laser beams for which the first echo is displayed in red and the last one in blue. The resulting pixel in the produced DSM is shown in the lower part of the figure. The cells A and B belong to the DSM. Generally, if two points belong to the same DSM cell and have the same X and Y coordinates, then the DSM cell value is equal to the mean altitude value of the two points. If Z_{Fi} and Z_{Li} represent the altitudes of the first and last reflection of laser beam number i, then the values of the cells A and B in DSM_{FE} and DSM_{LE} are calculated as follows:

$$DSM_{FE} (A) = (Z_{F1} + Z_{F3}) / 2, \qquad (2)$$

$$DSM_{FE} (B) = Z_{F2}, \qquad (3)$$

$$DSM_{LE} (A) = Z_{L3}, \qquad (4)$$

$$DSM_{LE} (B) = (Z_{L1} + Z_{L2}) / 2. \qquad (5)$$

Consequently, the values of these cells in the DIF matrix are:

$$DIF (A) = (Z_{F1} + Z_{F3}) / 2 - Z_{L3} > 0, \qquad (6)$$

$$DIF (B) = Z_{F2} - (Z_{L1} + Z_{L2}) / 2 < 0. \qquad (7)$$

Therefore, it is clear that DIF (B) is inferior to zero. Moreover, the accuracy difference between the first and the last echo sometimes generates negative values in the DIF matrix.
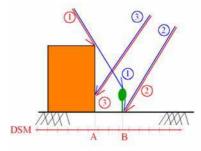

Figure 3: Explanation of negative values in the DIF matrix. First echo is marked in red and last echo in blue.

4.2.2 Extension of the algorithm to the use of first and last echo: Like the original approach, this procedure starts with the segmentation of terrain and off-terrain points. Since this processing step is identical to the first step of the original algorithm it is not explained again in this part.

The second step of the process consists in the discrimination of the off-terrain class into the subclasses vegetation and

buildings. This is the point where the modified approach differs from the original one. In this adapted and extended method, first of all, the difference between first and last echo DSM is calculated and provides the DIF matrix (as shown in the previous section). The DIF matrix is an indicator for the nature of the pixels (vegetation or building) and is consequently useful for the elimination of a large part of vegetation. Indeed, as already mentioned, pixels having values equal to zero in the DIF matrix represent terrain and building bodies; furthermore, pixels with other values represent vegetation and building borders. So the off-terrain pixels corresponding to non-zero pixels of the DIF matrix have to be eliminated. In order to remove the remaining vegetation segments considered as noise, the threshold S limiting the minimal acceptable building surface is introduced. In such a manner the noisy building kernel mask can be cleaned and then the remaining segments represent the building kernels. The last step of this building extraction task consists in completing the building kernels with the surrounding pixels lost previously. This is done with the use of a normalised first echo DSM on which the same region growing algorithm is applied as it is used during the original approach (see section 4.1). It works on the eight neighbouring height differences (Δh_{roof}). A last filter operation erases the remaining segments by regarding the threshold S again.
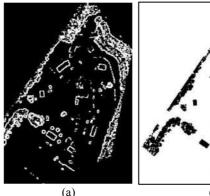
5. RESULTS AND COMPARISON OF THE TWO APPROACHES

5.1 Detection of the off-terrain class

The segmentation of the point cloud into terrain and off-terrain points works identically for both algorithms. It starts with the detection of the off-terrain boundaries as described in section 4.1. The results obtained for this processing step are shown in Figure 4(a).

In order to describe the quality of the building boundary detection, three qualifiers are defined:

> *all*:   the whole building boundary is detected
> *some*: only parts of the building boundary are detected
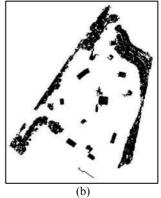> *any*:   the whole building boundary is not detected

(a)   (b)

Figure 4: a) Detection of the off-terrain class borders (Δh=3 m). b) Detected off-terrain objects (Δh=3 m and S=75 m²).

There are several reasons that explain why some building boundaries are detected only partially:

1. The height difference between the building boundary and the neighboured ground is smaller than the threshold Δh representing the minimum height difference between terrain and off-terrain (Figure 5(a)).
2. One or more facades of the building are inclined (Figure 5(b)).
3. There is an obstacle near the building making the altitude difference between the building and its neighboured ground smaller than threshold Δh (Figure 5(c)).
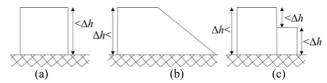

(a)   (b)   (c)

Figure 5: Three cases for the non-detection of building boundaries: a) Building with a height smaller than Δh. b) Building with an inclined facade. c) Building with an obstacle in the vicinity.

Building number	Damage type	Style of roof	Building boundary detection	Reason for non-detection	Detection	Only first echo	First and last echo
1a	pancake collapse, all stories	flat roof	*some*	1	*dis*	detected	detected
1b	pancake collapse, all stories	flat roof	*some*	1	*par*	detected	detected
2	pancake collapse in combination with an inclination	flat roof	*some*	1	*par*	detected	undetected
3	inclined plane	flat roof	*some*	1	*par*	undetected	undetected
4	undamaged	flat roof	*all*	-	*com*	detected	detected
5	undamaged	flat roof	*all*	-	*com*	detected	detected
6a	undamaged	barrel-shaped roof	*some*	3	*com*	detected	detected
6b	pancake collapse, all stories	flat roof	*some*	1	*com*	detected	undetected
7	undamaged	flat roof	*all*	-	*com*	undetected	undetected
8	undamaged	gabled roof	*all*	-	*com*	detected	detected
9	undamaged	barrel-shaped roof	*some*	3	*par*	undetected	undetected
10	undamaged	gabled roof	*some*	3	*com*	undetected	undetected
11	undamaged	gabled roof	*some*	3	*com*	detected	detected

Table 2: Characteristics of the buildings and results of the single processing steps

Table 2 presents the results of the boundary detection. It can be seen that the boundaries of 4 buildings (all undamaged) are detected completely, whereas the boundaries of 9 buildings (5 damaged and 4 undamaged) are detected only partially.

After the off-terrain boundaries, the bodies of the off-terrain objects are determined (Figure 4(b)). For describing the quality of the building detection during the extraction of the off-terrain class the following three qualifiers are used:

com: building is detected completely
par: building is detected partially
dis: building is not detected at all

The results of this processing step are also summarised in Table 2. It can be noticed that 8 buildings are detected entirely. Four of them correspond to the buildings for which the whole boundary was extracted in the previous step.

The buildings 6a, 6b, 10 and 11 are determined because the missing boundary parts are small enough. As a consequence, it can be pointed out that the results of this step are directly correlated with the results of the off-terrain boundary detection. If the boundary of a building is completely detected, the whole building body will be extracted as well. Else its detection is dependent on the orientation of the building in relation to the direction of the moving window.

5.2 Extraction of buildings from the off-terrain class

Figures 6(a) and 6(b) show the results obtained by using the original and the extended algorithm, respectively. Table 2 gives an overview of the final results.
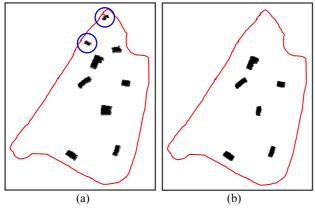

(a)   (b)

Figure 6:   a) Building detection using DSM and first echo only. b) Building detection using first and last echo.

If the original approach using first echo only is applied to the test dataset, 9 buildings are detected correctly, whereas 4 buildings remain undetected. That means that 4 of the 5 damaged and 5 of the 8 undamaged buildings can be found. The reason for the non-detection of the buildings 3, 7, 9 and 10 is their size. Their building kernels determined during the second step of the process (see section 4.1) are smaller than threshold *S* standing for the minimal building size. That is the case because there are details and noise on the roof surfaces. Furthermore, the nature of the building roofs plays an important role at the extraction of buildings, because the algorithms act on the assumption that roofs are generally composed of planar surfaces. If this assumption is not fulfilled, like e.g. for building 9, the algorithms fail for the concerning building. Furthermore,

there are two cases in which misclassifications occur i.e. vegetation is classified as building. They are marked in Figure 6(a) with blue circles.

The use of the extended method introducing first and last echo as input data results in the detection of the buildings 1a, 1b, 4, 5, 6a, 8 and 11. That means that besides the buildings which have not been extracted by the original algorithm the buildings 2 and 6b stay undetected additionally. The buildings 3, 7, 9 and 10 are not identified because of the same reasons as described above for the other method. Concerning the buildings 2 and 6b it has to be mentioned that they are damaged. In the case of damaged buildings there is the risk of eliminating supplementary points over the building roof if the DIF matrix is used for the elimination of vegetation. Consequently, the building kernels are smaller than those obtained by using first echo data only.

Building 1a is extracted by both methods although it has not been detected as off-terrain object in the first step of the algorithms (see section 5.1). For understanding this phenomenon, it has to be mentioned that there are two possibilities for the input data of the region growing algorithm:

1.   The region growing algorithm is based on the total DSM. In this case the possibility exists to complete the disappeared parts of only partially detected buildings. At the same time, if the used height difference threshold Δh_{roof} is relatively big and the terrain and off-terrain separation threshold Δh is relatively small, the risk exists that all points of the DSM are detected as off-terrain.
2.   The region growing algorithm is applied on the off-terrain class. In this case there is not any risk, but the partially detected buildings cannot be completed.

In the studied examples, the region growing algorithm is based on the total DSM, because the used height difference threshold Δh_{roof} was small (Δh_{roof}=0.35 m). Now it is obvious that building 1a is correctly detected since it is adjacent to building 1b.

6.   CONCLUSION AND FUTURE WORK

It has to be noted that the results obtained by using first echo only are more satisfactory than those achieved by using both first and last echo, since the number of buildings detected by this segmentation is higher (see Figures 6(a) and 6(b), Table 2). On the other hand, the obtained results achieved by the extended algorithm are more satisfying in areas where the proportion of vegetation is high. Consequently, in general case, if both echoes are available, it would be judicious to carry out the calculation by applying both algorithms and by preserving the union of the images extracted in this way. However, in the presented example no improvement could be achieved by generating the union of the two images because the extended method does not detect additional buildings. Furthermore, the vegetation classified as buildings by the original algorithm would not be eliminated.

It has been shown in which cases undamaged buildings as well as damaged buildings can be detected by the developed approaches. To recapitulate, it can be said that the results depend strongly on the thresholds used for the minimal height differences and the minimum building surfaces. As a consequence, buildings lower than the height difference

threshold Δh or smaller than the minimum building surface S cannot be identified, no matter if they are damaged or not. Therefore, damaged buildings can only be detected if they exceed a certain height. A further condition for their recognition is that the roof structure is preserved and that its slope is lower than the threshold value of the maximum allowed roof slope (Δh_{roof}). So the assumption was confirmed that only buildings suffered by damage types like *pancake collapses*, *inclined planes* or *overhanging elements* can be extracted. In contrary damage types like all *heaps of debris* types or *outspread multi layer collapses* remain undetected.

In the near future, both institutes will follow up their research in order to construct 3D building models automatically allowing the realisation, classification and quantification of the total building damages. For this purpose, a terrestrial laser scanning campaign was carried out on the test area in March 2007. On the one hand, it shall be used to confirm these results and on the other hand, it will provide useful data for completing the 3D models of the buildings.

REFERENCES

Alharthy, A. and Bethel, J., 2002. Heuristic filtering and 3d feature extraction from LIDAR data. In: *International Archives of Photogrammetry and Remote Sensing (IAPRS)*, Graz, Austria, Vol. XXXIV, Part 3A, ISSN 1682-1750, pp. 29-34.

Alharthy, A. and Bethel, J., 2004. Detailed building reconstruction from airborne laser data using a moving surface method. In: *IAPRS*, Istanbul, Turkey, Vol. XXXV, Part B3.

Dash, J., Steinle, E., Singh, R.P. and Bähr, H.-P., 2004. Automatic building extraction from laser scanning data: an input tool for disaster management. *Advances in Space Research*, Volume 33, Issue 3, pp. 317-322.

Hyyppä, H., Yu, X., Hyyppä, J., Kaartinen, H., Kaasalainen, S., Honkavaara, E. and Rönnholm, P., 2005. Applicability of first pulse derived digital terrain models for boreal studies. In: *The International Archives of Photogrammetry, Remote Sensing and Spatial Information Sciences (IAPRSIS)*, Enschede, The Netherlands, Vol. XXXVI, Part 3/W19, ISSN 1682-1777.

Kraus, K., and Pfeifer, N., 1998. Determination of terrain models in wooded areas with airborne laser scanner data. *ISPRS Journal of Photogrammetry and Remote Sensing*, 53, pp. 193-203.

Lee., I. and Schenk., T., 2002. Perceptual organization of 3d surface points. In: *IAPRS*, Graz, Austria, Vol. XXXIV, Part 3A, ISSN 1682-1750, pp. 193-198.

Lohmann, P., Koch, A. and Schaeffer, M., 2000. Approaches to the filtering of laser scanner data. In: *IAPRS*, Amsterdam, The Netherlands, Vol. XXXIII, Part B3/1, pp. 534-541.

Murakami, H., Nakagawa, K., Shibata, T. and Iwanami, E., 1999. Potential of an airborne laser scanner system for change detection of urban features and orthoimage development. In: *IAPRS*, Stuttgart, Germany, Vol. XXXII, Part 4, pp. 422-427.

Pfeifer, N., Reiter, T., Briese, C. and Rieger, W., 1999. Interpolation of high quality ground models from laser scanner data in forested areas. In: *IAPRS*, La Jolla, California, USA, Vol. XXXII, Part 3-W14, pp. 31-36.

Rehor, M. and Bähr, H.-P., 2006. Segmentation of damaged buildings from laser scanning data. In: *IAPRSIS*, Bonn, Germany, Vol. XXXVI, Part 3, ISSN 1682-1750, pp. 67-72.

Rottensteiner, F. and Briese, Ch., 2002. A new method for building extraction in urban areas from high-resolution LIDAR data. In: *IAPRS*, Graz, Austria, Vol. XXXIV, Part 3A, ISSN 1682-1750; pp. 295-301.

Schweier, C. and Markus, M., 2004. Assessment of the search and rescue demand for individual buildings. In: *Proceedings of the 13th World Conference on Earthquake Engineering*, Vancouver, Canada.

Tarsha-Kurdi, F., Landes, T., Grussenmeyer, P. and Smigiel, E., 2006. New approach for automatic detection of buildings in airborne laser scanner data using first echo only. In: *IAPRSIS*, Bonn, Germany, Vol. XXXVI, Part 3, ISSN 1682-1750, pp. 25-30.

Tarsha-Kurdi, F., Landes, T. and Grussenmeyer, P., 2007. Joint combination of point cloud and DSM for 3D building reconstruction using airborne laser scanner data. *6th International Symposium on Remote Sensing of Urban Areas*, Paris, France.

Tóvári, D. and Vögtle, T., 2004. Classification methods for 3D objects in laserscanning data. In: *IAPRS*, Istanbul, Turkey, Vol. XXXV, Part B3, ISSN 1682-1750.

Vu, T.T., Matsuoka, M. and Yamazaki, F., 2004a. LIDAR-based Change Detection of Buildings in Dense Urban Area. In: *Proceedings of the International Geoscience and Remote Sensing Symposium, IEEE*, Anchorage, Alaska, USA, CD-ROM, pp. 3412-3416.

Vu, T.T., Matsuoka, M. and Yamazaki, F., 2004b. Employment of LIDAR in Disaster Assessment. In: *Proceedings of the 2nd International Workshop on Remote Sensing for Post-Disaster Response*, Newport Beach, California, USA.

Wotruba, L., Morsdorf, F., Meier, E. and Nüesch, N., 2005. Assessment of sensor characteristics of an airborne laser scanning using geometric reference targets. In: *IAPRSIS*, Enschede, The Netherlands, Vol. XXXVI, Part 3/W19, ISSN 1682-1777.

Wang, M. and Tseng, Y.-H., 2004. Lidar data segmentation and classification based on octree structure. In: *IAPRS*, Istanbul, Turkey, Vol. XXXV, Part B3, ISSN 1682-1750.

Yu, X., Hyyppä, H., Kaartinen, H., Hyyppä, J., Ahokas, E. and Kaasalainen, S., 2005. Applicability of first pulse derived digital terrain models for boreal studies. In: *IAPRSIS*, Enschede, The Netherlands, Vol. XXXVI, Part 3/W19, ISSN 1682-1777.